Spatio-temporal characterization of precipitation in the Middle and Lower Paraguay Basin based on satellite products and weather station data

Rossana Villalba, [1,2], Anabella Ferral [1], Julián Baéz [3], Jorge Kurita [2], Víctor Hugo Gauto [4], Juan Carlos Bertoni [5]

[1] Instituto Gulich, CONAE, Argentina - rvillalba@pol.una.py, aferral@conae.gov.ar
[2] National University of Asunción, Paraguay - gkurita@gmail.com
[3] Faculty of Science and Technology, Catholic University of Asunción, Paraguay - julian_baez@uc.edu.py
[4] National Technological University, Resistencia, Argentina - victor.gauto@ca.frre.utnedu.ar
[5] Faculty of Exact, Physical, and Natural Sciences, Argentina - jcbertoni@gmail.com

Keywords: IMERG, CHIRPS, El Niño, Validation, Accumulated precipitation, Anomalies

Abstract

This study presents a temporal analysis aimed at identifying climatic patterns that influence precipitation behavior in the Middle and Lower Paraguay Basin, part of the Paraná River Basin in Paraguayan territory. This research utilizes satellite-based geospatial technologies to analyze the spatial and temporal variability of precipitation in the region. Satellite precipitation images were used for the period 2001-2023, available on NASA's GIOVANNI platform. The results from the classical exploratory statistical analysis allowed for the identification of data distribution, spatial and temporal variability of precipitation in the basin, areas with the highest accumulations, and drought periods, as well as extreme events associated with the El Niño-Southern Oscillation (ENSO) phenomenon, which impacts southern tropical America, including Paraguay. Through the use of remote sensing data and geomatics techniques, this study supports the goals of GEM24, which focus on applying geospatial technologies to address environmental monitoring challenges. The average monthly precipitation series shows a steady trend, with a decrease in recent years. The lowest average was in August 2004 (5.6 mm), and the highest was in December 2015 (345.22 mm). December is the month with the highest average precipitation, while August records the lowest value. The validation between the precipitation data obtained from the Giovanni platform and conventional weather station data, through correlation and linear regression analysis, revealed a strong and statistically significant relationship, indicating that the satellite model is suitable for predicting precipitation, although not perfect. Additionally, the study of temporal anomalies identified prolonged drought periods (2001-2013 and 2020-2022), with intensification in 2020, and periods of intense rainfall (2014-2019), highlighting the 2015 floods. The spatial precipitation anomalies during El Niño (2015) and La Niña (2020), using IMERG and CHIRPS data, allowed for the identification of precipitation spatial patterns. The areas with the highest precipitation were concentrated in the east and south of the country, while drier areas, such as the Paraguayan Chaco in the basin (west), recorded lower precipitation. This study underscores the role of satellite data and geomatics in environmental monitoring, demonstrating how these technologies can enhance our understanding of climatic patterns and extreme weather events. The findings highlight the importance of geospatial data in global environmental change assessments and the monitoring of regional climatic variability, which are central to the objectives discussed in GEM24.

1. Introduction

The socio-environmental risks caused by droughts and floods in the Middle and Lower Paraguay Basin have not yet been evaluated. The lack of open data and local analyses in this basin limits the ability to adequately address the concept of risk, understood as vulnerability to hazards (Beltramone, 2017). There is an urgent need to characterize both vulnerability and threats over space and time, using precipitation behavior in the basin as an indicator to assess the hazard or threat, as it is directly related to floods and droughts (Huang, 2021). Globally, numerous studies have used remote sensing information to map and characterize precipitation in basins, especially in the study of flood and drought periods. However, no studies with a specific spatio-temporal focus on the Middle and Lower Paraguay Basin have been found, despite this region being affected by these problems in recent years, particularly during El Niño and La Niña events.

The El Niño-Southern Oscillation (ENSO) is a recurrent climate pattern involving changes in the temperature of central and eastern Pacific Ocean waters, as well as atmospheric pressure (Mishra, 2014). Few previous studies have addressed the characterization of streamflow and precipitation at the local level in this region (Puri, S., 2009) and (Mishra, 2014). Previous work has provided preliminary results on the relationship between precipitation and floods, highlighting the importance of having high spatial and temporal resolution data for more accurate characterization (Villalba, 2023).

Expanding this analysis to the spatial scale, as other authors have done in different basins, is essential to capture patterns that can contribute to risk planning and management in the basin. This study focuses on identifying one of the factors contributing to flood hazards: accumulated precipitation in the basin. The goal of the present study is to characterize, both spatially and temporally, the behavior of accumulated precipitation in the Middle and Lower Paraguay Basin during the period 2001-2023, using freely available remote sensing products and validating this information with local weather station data.

2. Methodos

2.1 Study Area

The study area is the Middle and Lower Paraguay Basin, which corresponds to the Paraguayan territory and the Plata Basin. Paraguay, located in the center of the South American continent, is characterized by a dense river network with three main rivers: the Pilcomayo River on the western border with Argentina, the Paraguay River, which runs through the central part of the country, and the Paraná River on the eastern border

with Brazil and Argentina. The Plata Basin covers territories of Argentina, Bolivia, Brazil, Uruguay, and the entirety of Paraguay (Puri, 2009).

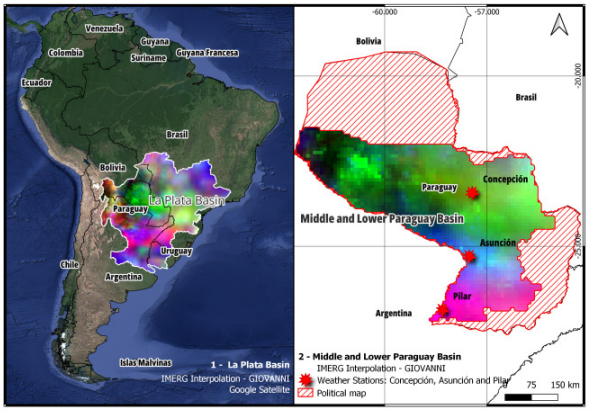

Figure 1. Shows the Middle and Lower Paraguay Basin within the Plata Basin, and Figure 1-2 shows the Middle and Lower Paraguay Basin corresponding to Paraguayan territory, with three meteorological stations (Concepción, Asunción, and Pilar). The interpolated precipitation analyses are based on IMERG data, corresponding to the average monthly precipitation from 2001 to 2023.

2.2 Satellites products

The product used was the GPM IMERG Final Precipitation L3 1 month 0.1 degree x 0.1 degree V07, Greenbelt, MD, from NASA's Goddard Earth Sciences Data and Information Services Center - GES DISC (http://disc.sci.gsfc.nasa.gov/). The Global Precipitation Measurement (GPM) IMERG products provide near-global satellite precipitation estimates, calculated using the 2021 version of the Goddard Profiling Algorithm (GPROF, 2021). These data are then gridded, intercalibrated with the GPM CORRA product (the Ku-band radar-radiometer combined algorithm), and merged into 0.1° x 0.1° fields (approximately 10 x 10 km) every half hour. This offers a database of remotely sensed information from sensors and analysis of rain gauges with accumulated monthly data through quasi-Lagrangian temporal interpolation. The precipitation phase is a diagnostic variable calculated through the analysis of surface temperature, humidity, and pressure (Huffman, 2023). In this study, GPM IMERG – V07 Final data was used, downloaded from NASA's Giovanni platform (https://giovanni.gsfc.nasa.gov). A total of 276 images corresponding to the average monthly precipitation from 2001 to 2023 for the Middle and Lower Paraguay Basin were downloaded, along with CHIRPS (Climate Hazards Group InfraRed Precipitation with Station data), downloaded from the Climate Hazards Group's infrared precipitation platform (https://data.chc.ucsb.edu/products/CHIRPS-2.0/), a quasi-global precipitation dataset. Spanning 50°S-50°N (and all longitudes) and covering the period from 1981 to the present., CHIRPS incorporates its internal climatology, CHPclim, satellite images at a 0.05° resolution, and in situ station data to create gridded rainfall time series for trend analysis and seasonal drought monitoring. CHIRPS uses advanced remote sensing techniques to integrate near-infrared and thermal satellite imagery, which captures key atmospheric information, especially in regions with sparse meteorological station coverage (Funk, 2022).

2.3 Meteorological Data

Average monthly precipitation data from three conventional meteorological stations were used, listed as follows: Aerodrome Concepción, Silvio Pettirossi Airport (Asunción), and Aerodrome Pilar. This information was provided by the National Civil Aviation Directorate (DINAC) through the Directorate of Meteorology and Hydrology of Paraguay, via official request.

2.4 Data Analysis

Data processing and map creation: the free software Rstudio, designed for statistical analysis and graphics (Moncayo Barahona, 2023), and QGIS – Geographic Information System, designed to create, edit, visualize, and analyze geospatial information (Montgomery, 2021), were used.

2.5 Validation of Precipitation Data

The validation between the precipitation data obtained from the Giovanni platform and the data from conventional meteorological stations was carried out in several steps to ensure the quality and accuracy of the satellite data. The following meteorological stations were considered: Concepción (57.43° S, 23.44° W), Asunción (57.51° S, 25.24° W), and Pilar (58.32° S, 26.88° W). First, the satellite data were temporally aligned with the meteorological station data. Then, the IMERG data were interpolated so that each grid or pixel matched the locations of the conventional meteorological stations. The station data were also checked, and missing values were completed using the mean method. At the start of the analysis, descriptive statistics (mean, median, standard deviation) were calculated, as well as the monthly and annual accumulated precipitation. Subsequently, a linear regression model was applied, a method used to fit a line that best explains the relationship between the two data sets. This model allowed the analysis of the correspondence between satellite precipitation and conventional meteorological station data. Through this adjustment, the relationship between both information sources was identified, evaluating the predictive capacity of the model and its accuracy. Equation 1 shows the Linear Regression model:

$$Y = \beta_0 + \beta_1 x \pm \varepsilon \quad (1)$$

where Y is the dependent variable, x is the independent variable, β_0 is the intercept, which represents the value of Y when x = 0, β_1 is the slope or regression coefficient, and ε is the residual error, which represents the difference between the observed value and the value predicted by the model (Okabe, A., 2009).The coefficient of determination (R^2), which measures the degree of fit of the linear regression model, was calculated. An R^2 close to 1 suggests a good model fit, meaning that satellite data can reliably predict the values recorded by the meteorological stations. Equation 2 is used to calculate the coefficient of determination (R^2):

$$R^2 = \frac{\sum_{i=1}^{n} (Y_{observed} - Y_{mean})^2}{\sum_{i=1}^{n} (Y_{observed} - Y_{predicted})^2} \quad (2)$$

where $Y_{observed}$ represents the observed values, and Y_{mean} is the mean of the observed values (Moncayo Barahona, 2023). The Residual Standard Error (RSE) was calculated to assess the variability in the data that is not explained by the linear

regression model. It represents the average magnitude of the residual errors, which are the differences between the observed values and the values predicted by the model. A lower RSE indicates higher accuracy of the model, as it corresponds to smaller prediction errors. This calculation serves to evaluate how well the model fits the data, complementing the analysis of R^2. The formula for the Residual Standard Error (RSE) is given in Equation 3

$$RSE = \sqrt{\frac{1}{n-p}\sum_{i=1}^{n}\left(Y_{observed,i} - Y_{predicted,i}\right)^2}, \quad (3)$$

where $Y_{observed}$ are the observed/reference values (stations), $Y_{predicted}$ are the estimated values (satellites), n is the number of observations, and p is the number of estimated parameters in the model (including the intercept) (Draper, N., 1998). Additionally, the results are visualized using scatter plots, line graphs, time series, and maps.

2.6 Calculation of Anomalies

To calculate the standardized monthly precipitation anomalies, Equation 4 is used for the standardized anomaly:

$$\text{Standardized Anomaly} = \frac{P_i - \overline{P}}{SD} \quad (4)$$

where P_i is the observed value, $\overline{P}$ is the mean of the series, and SD is the standard deviation (Montgomery, 2021). This allows observing patterns, trends, and anomalous events in the annual average precipitation in the Middle and Lower Paraguay Basin.

3. Results

3.1 Descriptive Statistics of the IMERG Time Series

After downloading the images, a time series was created from them, corresponding to the monthly average, maximum, minimum, and standard deviation of precipitation (in mm) obtained from the GIOVANNI platform. The lowest average recorded was in August 2004 (1.84 mm) and the highest monthly average was in December 2015 (345.22 mm). The series shows an apparently constant trend with a tendency to decrease. **Figure 2a** shows the average precipitation for the series. **Figure 2b** shows the minimum recorded precipitation, which can be observed in December 2003 (127.22 mm). **Figure 2c** shows the maximum monthly precipitation for the time series. The lowest maximum precipitation was observed in July 2017 (30.50 mm) and the highest in November 2009 (624.24 mm). **Figure 2d** shows the monthly standard deviations for the time series from 2001 to 2023. The highest standard deviation (136.39 mm) relative to the mean (345.22 mm) can be observed in December 2015.

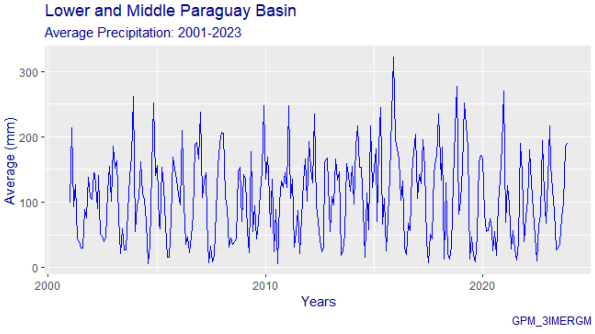

Figure 2a. Average monthly precipitation for 2001-2023 period in Lower and Middle Paraguay Basin.

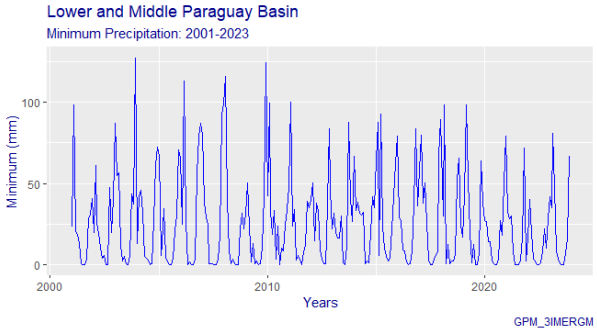

Figure 2b. Minimum monthly precipitation for 2001-2023 period in Lower and Middle Paraguay Basin.

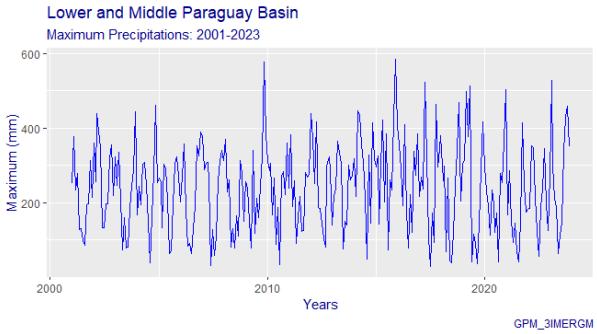

Figure 2c. Maximum monthly precipitation for 2001-2023 period in Lower and Middle Paraguay Basin.

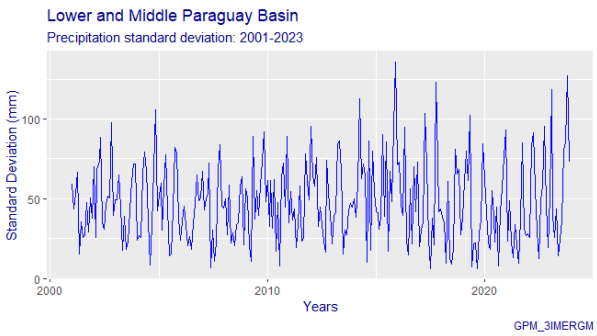

Figure 2d. Precipitation standard deviation for 2001-2023 period in Lower and Middle Paraguay Basin.

3.2 Temporal and Spatial Characterization of IMERG Data

In this section, we present monthly and annual analyses, including statistics and maps to examine the temporal and spatial patterns of IMERG data. We also provide an annual harmonization. Figure 3 shows box plots of the IMERG precipitation series based on each month. A consistent average with a downward trend in June, July, and August, and an upward trend in October, November, and December can be observed.

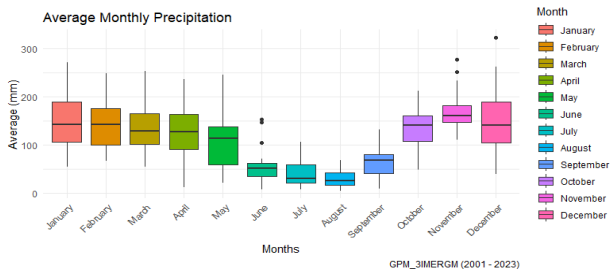

Figure 3. Precipitation boxplots for different months calculated over IMERG data for the period 2001-2003 in Lower and Middle Paraguay Basin.

Figure 4 presents the calculated statistics from IMERG products: average, maximum, minimum, and standard deviation. The results indicate that the average precipitation values are generally low, with a similarly low standard deviation, suggesting minimal variability in precipitation. This implies that rainfall events are typically consistent (and low), particularly in the Paraguayan Chaco region, highlighted in yellow in the northwest.

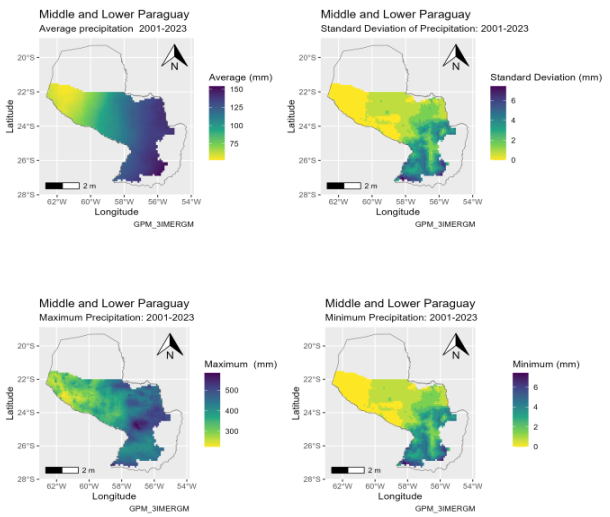

Figure 4. IMERG statistic calculated at a pixel level for the period 2001-2023 at the Lower and Middle Paraguay Basin. Top left: Average; Top-right: Standard Deviation; Bottom-left: maximum; Bottom-right: minimum.

Figure 5 presents annual precipitation anomalies, which help identify deviations from the long-term average. The years 2001, 2005, 2008, 2020, and 2021 show persistent precipitation deficits, while the years 2014 and 2015 exhibit precipitation surpluses.

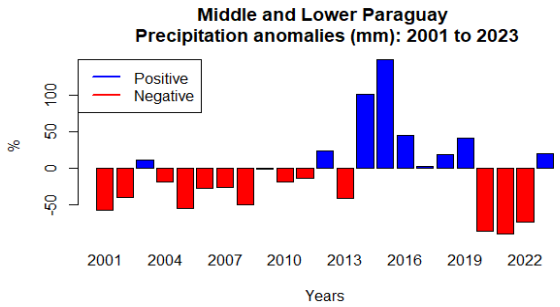

Figure 5. Annual precipitation anomalies calculated over IMERG data for the period 2001-2003 in the Lower and Middle Paraguay Basin.

Figure 6 presents annual precipitation maps from IMERG for the period 2001-2023. These graphs allow the analysis of the annual precipitation behaviour in time and space, where each pixel represents the average amount of rainfall during each year. It can be observed that the average precipitation is minimal for almost all the years, with minimum values close to zero. These indicators show that the region experienced persistent precipitation scarcity, particularly accentuated in the western, drier side (yellow), while there is a higher probability of precipitation in the eastern-southern, wetter side (blue).

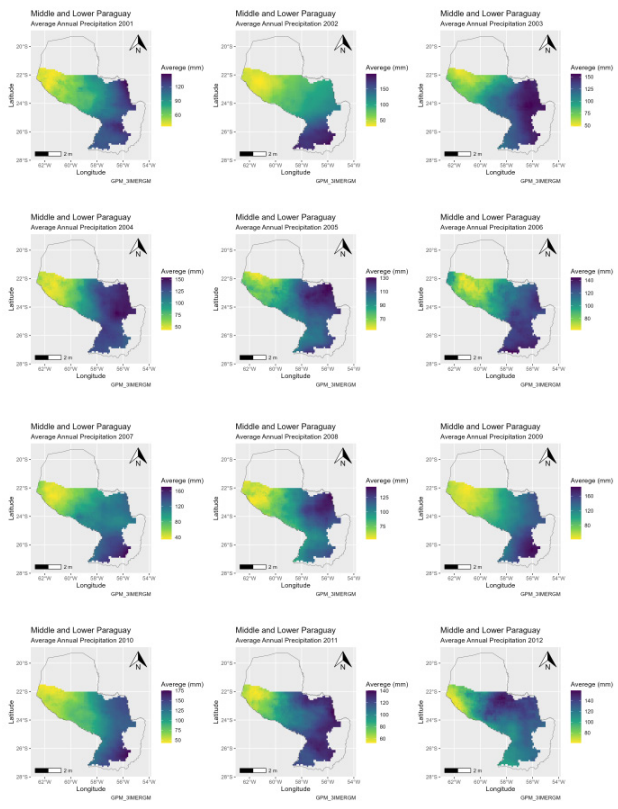

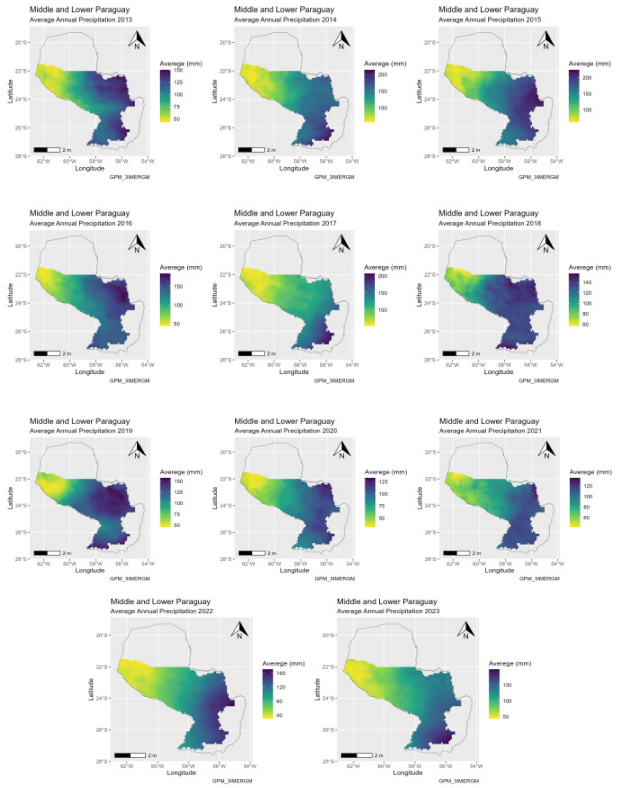

Figure 6. IMERG average precipitation maps for the period 2001-2023. Each map represents the annual average of monthly IMERG data downloaded from GIOVANI/NASA platform.

3.3 Validation and Comparison with Weather Stations

For validation purposes, the precipitation averages calculated from satellite data (IMERG) were compared with data from conventional weather stations located in Concepción, Asunción and Pilar. This process allowed for the validation of the accuracy of the satellite data and the adjustment of linear regression models. Figure 3-9 shows the regression model between IMERG monthly average precipitation data and monthly precipitation data measured in the Asunción meteorological weather station. The obtained fit is quite strong, with an adjusted R^2 of 0.89, suggesting that nearly 89% of the variability in Y (IMERG data) is explained by x (meteorological data precipitation). The Residual Standard Error (RSE), which measures the average distance of the data points from the values predicted by the model, indicates that, on average, individual data points are 28.47 units away (mm) from the value predicted by the regression equation. The calculated p-value, which indicates the significance of the relationship between the variables, is less than 2.2 x 10-16. This extremely small value (less than 0.05, in this case) suggests that the relationship is highly significant and that the model fits the observed data well. Figure 3-10 shows the regression model between IMERG monthly average precipitation data and monthly precipitation data measured in the Concepción meteorological weather station. It can be observed an adjusted R^2 of 0.90 (90%), indicating that the model has an efficient fit, with no evidence of overfitting. The Residual Standard Error (RSE) indicates that, on average, the values predicted by the model have an error of 27.49 mm; a lower RSE suggests a better fit. The p-value < 2.2 x 10-16 confirms that the relationship between the variables is highly significant. **Figure 7** shows the regression model between IMERG monthly average precipitation data and monthly precipitation data measured in the Pilar weather station. The adjusted R^2 value of 0.84 (84%) suggests that the model is good and efficient, with little overfitting. The Residual Standard Error (RSE) of 35.83 mm reflects the model’s precision. The p-value < 2.2e-16, extremely low, reinforces that the relationship between the variables is also statistically significant.

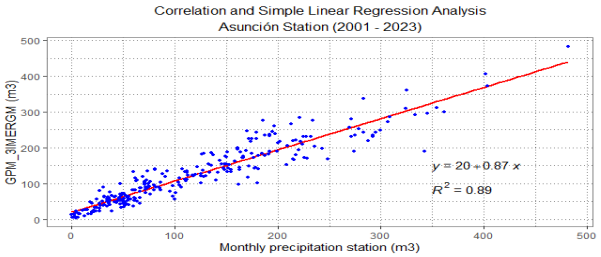

Figure 7a. Regression model between IMERG monthly average precipitation data and monthly precipitation data measured in Asunción meteorological weather station.

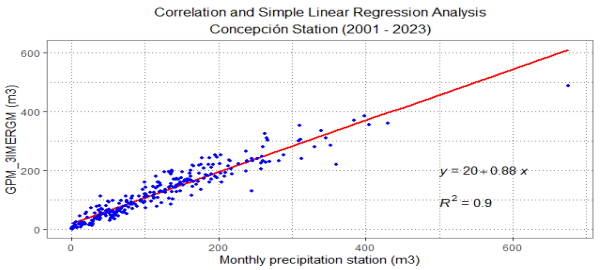

Figure 7b. Regression model between IMERG monthly average precipitation data and monthly precipitation data measured in Concepción meteorological weather station.

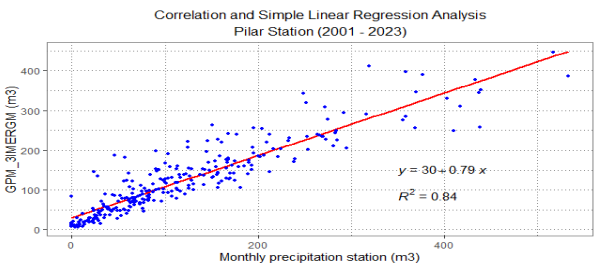

Figure 7c. Regression model between IMERG monthly average precipitation data and monthly precipitation data measured in the Pilar meteorological weather station.

3.4 Spatial Anomaly Characterization during El Niño (2015) and La Niña (2020) Events Using IMERG Data

Given the annual anomalies identified for 2015 and 2020 in Figure 8, which correspond to El Niño and La Niña years, respectively (Villalba, 2023, November), spatial precipitation patterns from IMERG were characterized for those years. It can be observed that precipitation levels exceed normal levels (106 mm). The spatial patterns highlight areas with higher precipitation than the expected normal values (blue). On the same map, positive anomalies range from 200 mm to 500 mm above the monthly mean, primarily in the southeastern region. Minimum precipitation values range from zero to 70 mm. Figures 8a and 8b present statistical precipitation maps for 2015 (El Niño) and 2020 (La Niña) in the Middle and Lower Paraguay Basin. For 2020, a negative precipitation anomaly pattern is observed in Figure 5. This year clearly shows drought

conditions, with precipitation dropping up to 100 mm below the monthly averages.

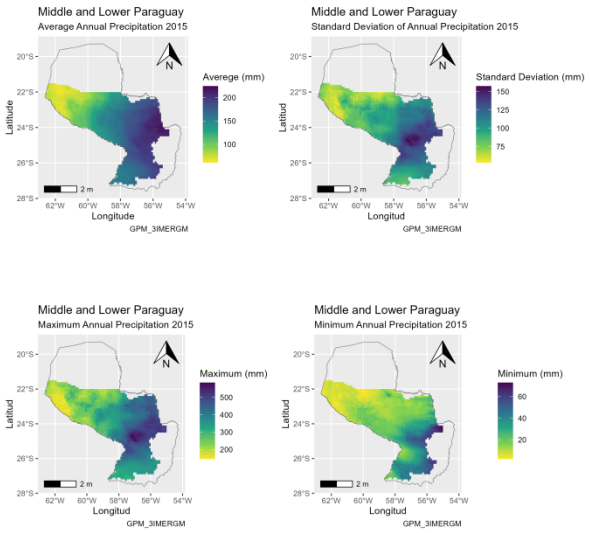

Figure 8a. IMERG precipitation statistical maps for 2015 (El Niño) year in the Lower and Middle Paraguay Basin, Top left: Average; Top-right: Standard Deviation; Bottom-left: maximum; Bottom-right: minimum.

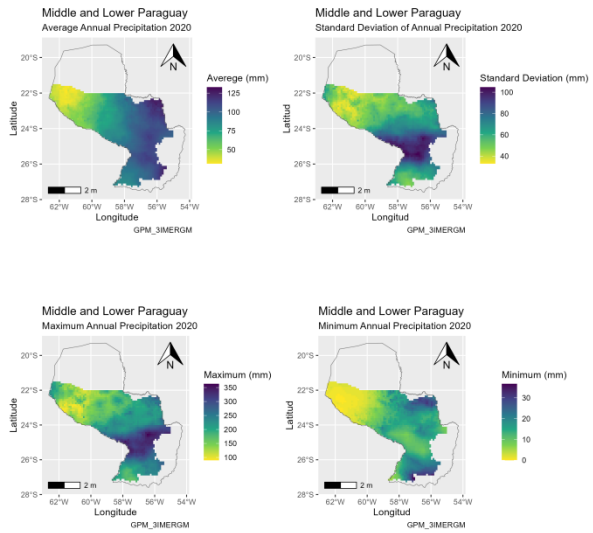

Figure 8b. IMERG precipitation statistical maps for 2020 (La Niña) year in the Lower and Middle Paraguay Basin, Top left: Average; Top-right: Standard Deviation; Bottom-left: maximum; Bottom-right: minimum.

3.5 Application of Remote Sensing Techniques with CHIRPS Data

A time series analysis was conducted to monitor precipitation using CHIRPS data from 1981 to 2023 in the Lower and Middle Paraguay Basin. The CHIRPS dataset integrates satellite imagery with in situ station data to provide high-resolution precipitation estimates, making it a reliable source for long-term climate analysis. The time series anomaly was calculated to monitor the interannual variability of precipitation, allowing for the identification of deviations from the long-term mean. This method enabled the detection of droughts, floods, and other extreme events over time. Additionally, IMERG (Integrated Multi-satellitE Retrievals for GPM) data, which combines information from multiple satellites within the Global Precipitation Measurement mission, was used for the period 2001-2023. IMERG provides high temporal and spatial resolution precipitation data, enabling detailed analysis of precipitation events and their spatial distribution. The anomalies calculated from IMERG data revealed climatic patterns consistent with those observed from CHIRPS data, providing a complementary perspective on interannual variability and reinforcing the reliability of the findings.

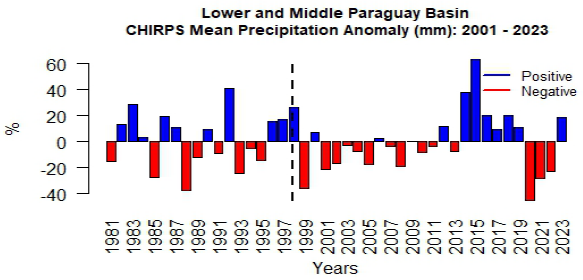

Figure 9. Annual precipitation anomalies calculated from CHIRPS data for the period 2001-2023 in the Bajo and Medio Paraguay Basin.

Using quantiles, the years with the lowest precipitation (droughts) and the highest precipitation (floods) in relation to the average were identified. From the study period (2001-2023), it was determined that the year 2020 was the driest, while the wettest year was 2015.

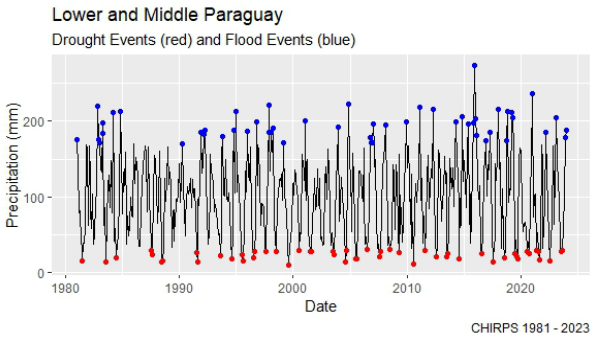

Figure 10. Identification of extreme events such as droughts and floods from CHIRPS data for the period 2001-2023 in the Lower and Meddle Paraguay Basin.

The following are the maps illustrating the flood event for December 2015, with an average precipitation of 196 mm, and the drought event in September 2020, with an average precipitation of 22 mm, based on CHIRPS data.

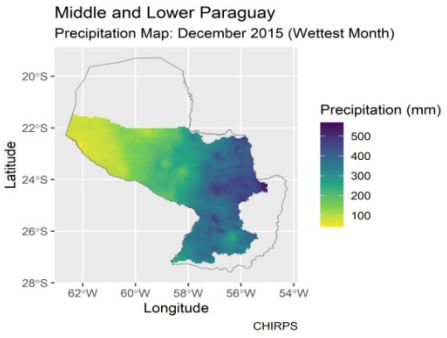

Figure 11. December 2020, the month with the highest precipitation, based on CHIRPS data for the period 2001-2023 in the Lower and Meddle Paraguay Basin.

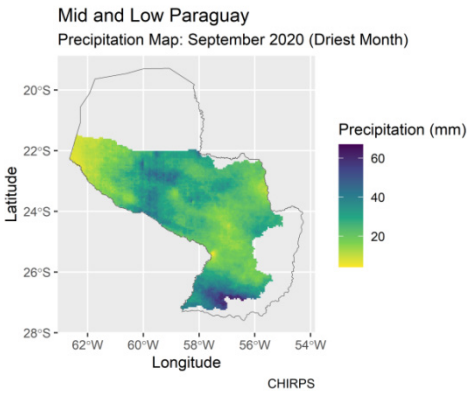

Figure 12. September 2020, the month with the lowest precipitation, based on CHIRPS data for the period 2001-2023 in the Lower and Meddle Paraguay Basin.

4. Conclusion

An analysis of the spatiotemporal precipitation patterns in the Lower and Middle Paraguay Basin, focusing on the Paraguayan territory, was conducted using satellite products and data from meteorological stations. The results reveal a generally constant average behavior influenced by periodic patterns. The descriptive analysis of the satellite data allowed for the identification of the wettest months (November 2009 and December 2015) and the driest months (September 2020 and August 2021). The maximum precipitation was recorded in December 2015 (584.78 mm) and November 2009 (576.00 mm). The relationship between the satellite data (IMERG) and meteorological stations is strong and statistically significant. The correlation and linear regression analysis indicate that the IMERG precipitation product is suitable for predicting precipitation with good, though not perfect, accuracy, with RMSE values ranging from 27.4 to 35.8 mm. The study of temporal anomalies identified prolonged droughts (2001-2013 and 2020-2022), with a notable intensification in 2020, as well as periods of intense rainfall (2014-2019). The results obtained, based on IMERG and CHIRPS data, show that for the time series between 2001 and 2023, the anomaly calculations have presented very similar results. The driest year identified was 2020, and the wettest year was 2015. Additionally, drought and wetness patterns have been detected from CHIRPS data. As a result of this analysis, two maps have been created: one corresponding to the driest month, September 2020, and the other to the wettest month, December 2015. These results will help improve the understanding of climatic variability in the region, in the face of extreme events related to climate change that could have a significant impact on local communities and the region's economy. Hydrologically, there is a concordance between the spatial patterns derived from satellite information and the point measurements from meteorological stations, suggesting that the results of the analysis reflect the influence of the ENSO phenomenon. Furthermore, this study highlights the utility of remote sensing techniques and satellite platforms such as IMERG and CHIRPS. These tools provide high-resolution spatiotemporal data that enable comprehensive climate monitoring, even in regions with limited ground-based meteorological infrastructure. By integrating satellite imagery with in situ data, the study leveraged advanced geospatial analysis techniques to enhance the understanding of precipitation dynamics. This combination underscores the importance of remote sensing technologies in addressing environmental challenges, supporting risk assessment, and improving water resource management in vulnerable regions like the Lower and Middle Paraguay Basin.

5. References

Bartholomew, D. J. (1971). Análisis de series de tiempo, pronóstico y control.

Beltramone, G., Alaniz, E., Ferral, A. E., Aleksinko, A., Arijón, D. R., Bernasconi, I., ... & Ferral, A. (2017, septiembre). Mapeo de riesgos de áreas urbanas propensas a inundaciones repentinas en cuencas montañosas utilizando el proceso analítico jerárquico y sistemas de información geográfica. En 2017 XVII Taller sobre procesamiento y control de información (RPIC) (pp. 1-6). IEEE.

Draper, N. (1998). Análisis de regresión aplicada. McGraw-Hill. Inc.

Funk, C. C., Peterson, P., Huffman, G. J., Landsfeld, M. F., Peters-Lidard, C., Davenport, F., ... & Husak, G. J. (2022). Introducing and Evaluating the Climate Hazards Center IMERG with Stations (CHIMES).

Huang, H., Cui, H., & Ge, Q. (2021). Evaluación de los riesgos potenciales inducidos por el aumento de las precipitaciones extremas en el contexto del cambio climático. Natural Hazards, 108(2), 2059-2079.

Huffman, G. J., Bolvin, D. T., Joyce, R., Kelley, O. A., Nelkin, E. J., Portier, A., ... & West, B. J. (2023). Notas de la versión de IMERG V07.

Mishra, V., Shah, R., & Thrasher, B. (2014). Sequías de humedad del suelo en el clima retrospectivo y proyectado en la India. Journal of Hydrometeorology, 15(6), 2267-2292.

Montgomery, D. C., Peck, E. A., & Vining, G. G. (2021). Introducción al análisis de regresión lineal. John Wiley & Sons.

Moncayo Barahona, E. L. (2023). Análisis de QGIS cómo plataforma tecnológica de soporte al procesamiento de datos geográficos relacionados con la agricultura en el cantón Pueblovieyo (Tesis de licenciatura, Babahoyo: UTB-FAFI. 2023).

Morales-Velázquez, M. I., Herrera, G. D. S., Aparicio, J., Rafieeinasab, A., & Lobato-Sánchez, R. (2021). Evaluación de reanálisis y precipitación satelital a escala regional: un estudio de caso en el sur de México. Atmósfera, 34(2), 189-206.

Okabe, A., Boots, B., Sugihara, K., & Chiu, S. N. (2009). Teselaciones espaciales: conceptos y aplicaciones de los diagramas de Voronoi.

Puri, S., & Aureli, A. (2009). Atlas de acuíferos transfronterizos: mapas globales, cooperación regional e inventarios locales.

Suriano, M., & Seoane, R. Variabilidad climática natural y su impacto en el río Paraná y Paraguay.

Villalba, R., Ferral, A., Baez, J., Kurita, J., Beltramone, G., & Bertoni, J. C. (2023, noviembre). Análisis temporal de la precipitación en la cuenca baja y media del Paraguay dentro de la cuenca del Plata (2001-2020) y su relación con el fenómeno El Niño/Oscilación del Sur (ENSO). En 2023 XX Taller sobre Procesamiento y Control de Información (RPIC) (pp. 1-6). IEEE.